

DNA Polymerase Locks Replication Fork Under Stress

Xiaomeng Jia^{1,2}, James T. Inman^{1,2}, Anupam Singh³, Smita S. Patel³, and Michelle D. Wang^{1,2,*}

¹Howard Hughes Medical Institute, Cornell University, Ithaca, NY 14853, USA

²Department of Physics & LASSP, Cornell University, Ithaca, NY 14853, USA

⁴Department of Biochemistry and Molecular Biology, Robert Wood Johnson Medical School, Rutgers University, Piscataway, NJ, USA

*Correspondence: mwang@physics.cornell.edu

Replication of DNA requires the parental DNA to be unwound to allow the genetic information to be faithfully duplicated by the replisome. While this function is usually shared by a host of proteins in the replisome, notably DNA polymerase (DNAP) and helicase, the consequence of DNAP synthesizing DNA while decoupled from helicase remains not well understood. The unwinding of downstream DNA poses significant stress to DNAP, and the interaction between DNAP and the replication fork may affect replication restart. In this work, we examined the consequences of DNAP working against the stress of the DNA replication fork. We found that prolonged exposure of DNAP to the stress of the replication fork inactivates replication. Surprisingly, replication inactivation was often accompanied by a strong DNAP interaction with the leading and lagging strands at the fork, locking the fork in place. We demonstrated that fork locking is a consequence of DNAP forward translocation, and the exonuclease activity of DNAP, which allows DNAP to move in reverse, is essential in protecting the fork from inactivation. Furthermore, we found the locking configuration is not reversible by the subsequent addition of helicase. Collectively, this study provides a deeper understanding of the DNAP-fork interaction and mechanism in keeping the replication fork active during replication stress.

DNA synthesis during replication is a highly dynamic process carried out by DNA polymerase (DNAP) in coordination with several other components within the replisome, such as helicase. Ideally, DNAP and helicase move synchronously at the replication fork, with helicase unwinding the DNA at the fork to allow DNAP access to the leading strand for replication. However, sometimes, this synchronization is disrupted. For example, if helicase lags behind DNAP or temporarily dissociates from the fork, the two separated DNA strands can re-anneal, leading DNAP to work against the fork on its own. DNAP must overcome the physical barriers of unwinding the fork to continue synthesizing the new DNA strand. This leads to replication stress, which can pose significant challenges to the replication machinery.

Understanding how DNAP responds to these conditions is crucial for elucidating the mechanisms maintaining genomic stability during DNA replication.

The ability of DNAP to function independently of helicase under these conditions remains an important question that is not fully understood. The T7 replisome is a model system for mechanistic understanding of replication¹⁻⁴ and serves as a simple model system to address this question. Previous studies show that when T7 DNAP encounters a DNA fork, it may replicate a few base pairs before stalling under the reannealing stress of the DNA in its front, which pushes the DNAP to move in reverse^{5,6}. DNAP can backtrack by removing the replicated DNA via its exonuclease activity, releasing the replication stress, which may provide a new opportunity for DNAP to forward translocate to replicate DNA. Thus, DNAP can shuttle between active replication and exonuclease activity during such stalling⁷. This stalling behavior raises questions about the enzyme's efficiency in restarting replication once replication stress is alleviated. However, little is known about how stalling impacts the ability of DNAP to restart due to a lack of complete understanding of the nature of DNAP's interaction with the replication fork.

This work aims to explore T7 DNAP's interactions with the replication fork and investigate the impact of replication stress on the enzyme's ability to resume DNA synthesis. We discovered a surprising behavior of DNAP's interaction with the fork. When DNAP works at the fork on its own for a prolonged duration, it can lock the fork by interacting with both the leading and lagging strands. Once locked, the fork cannot be unlocked readily as DNAP binds tightly to the fork, even after helicase addition. Fork-locking results from DNAP synthesizing DNA while advancing the fork without helicase. Interestingly, the exonuclease activity of DNAP is essential to minimizing fork locking, revealing a new role of exonuclease in maintaining an active fork. These results on how the basal replication machinery DNAP interacts with a replication fork may have significant implications for understanding replication stalling and subsequent replication restart.

Results

DNAP can lock the replication fork

If T7 DNAP interacts with a replication fork for an extended duration, DNAP cannot replicate a substantial distance as the fork represents a significant resistance to DNA replication. This raises the possibility that this resistance may inactivate the bound DNAP. To investigate this possibility, we employed two techniques that we previously developed⁸⁻¹¹ to study protein-DNA interactions via mechanical unzipping of a DNA molecule using an optical

trap (Fig. 1a, Fig. S1b). The “unzipping tracker” uses the DNA fork to track the trajectory of a translocating motor in real-time, and the “unzipping mapper” detects the location and strength of a bound protein via rapid mechanical unzipping through the bound protein.

In this experiment, we first incubated replication forks (Fig. S1a) with T7 DNAP for a specified duration. Subsequently, we used the unzipping tracker to examine whether a replication fork was still active by holding the fork at a force of 12 pN, which facilitates DNA unzipping and allow leading strand DNA synthesis without helicase^{3, 4, 12} (Fig. 1a,b). If a trace showed active replication, DNA extension increased by 0.77 nm for each nucleotide replicated (Methods). In contrast, inactive replication did not increase DNA extension.

Immediately following this step, we employed the unzipping mapper and rapidly unzipped through the remainder of the parental DNA to detect any interactions of DNAP with the parental DNA (Fig. 1a,c). We noticed that an active trace typically showed no force rise above the naked DNA baseline during the unzipping mapper step. Surprisingly, an inactive trace often showed a force rise significantly above the naked DNA baseline at the beginning of the unzipping. This force rise reveals that the fork experiences resistance to strand opening. Since such resistance was not present without DNAP, this finding suggests that a DNAP can simultaneously interact with both the leading and lagging strands at the fork, “locking” the fork and rendering it inactive.

We found a strong correlation between a fork's activity during the unzipping tracker step and the subsequent unzipping force rise during the unzipping mapper step: an inactive fork typically leads to a force rise (Fig. 1d). The average disruption force is about 27.2 pN, comparable to forces required to disrupt a bound *E. coli* RNA polymerase^{13, 14}, a Cas protein¹⁰, restriction enzymes^{11, 15, 16}, or a nucleosome¹⁷⁻²⁰, which can also be significant barriers to replication²¹⁻²³. Furthermore, we found that forks became increasingly less active with an increase in the incubation duration (Fig. 1e). To exclude the possibility that fork locking is a consequence of DNAP degradation at room temperature over the incubation period, we left the DNAP in a test tube without any DNA fork for 4 hours and tested its activity. We found that the DNAP activity remained unchanged (Fig.S2a). Thus, these data demonstrate that prolonged interaction of DNAP with a replication fork leads to DNAP locking and inactivation of the fork.

DNAP exonuclease activity limits fork-locking

Since T7 DNAP can support both polymerization activity and a 3' to 5' exonuclease activity, we first examined how the exonuclease activity impacted the observed DNAP fork-locking behavior. Thus, we repeated the experiments shown in Fig. 1 using two DNAP mutants

lacking exonuclease activity (Fig. 2, Fig.S3): one containing two point-mutations, which we refer to as *exo- DNAP*, and the other, *Sequenase*, which lacks the exonuclease domain.

After incubating the forks with these mutants for 90 min, we detected both active and inactive traces with these two enzymes (Fig. 2a). However, unlike WT DNAP, these enzymes often already replicated many nucleotides before the detection step (Fig. 2b). We found that WT DNAP replicated minimally, about 15 nt (Fig. 2b). In contrast, both *exo- DNAP* and *Sequenase* replicated about 170 nt (Fig. 2b). Thus, the inability to move in reverse facilitates the progression of these mutants to move against the fork, even without the assistance of helicase, consistent with previous findings²⁴⁻²⁶.

Significantly, the inactive fraction and the correspondingly locked forks increased dramatically from 15% for the WT DNAP to about 85-90% for the two mutants (Fig. 2c). In fact, the *exo- DNAP* and *Sequenase* required much less time to inactivate the fork, reaching this level of inactivity after only 30 minutes incubation (Fig. S4), significantly faster than that of WT DNAP. Our control experiments show that this difference was not due to DNAP degradation during incubation (Fig. S2b). Thus, while the inability to move in reverse facilitated forward movement for these mutants, this inability also made the enzyme more vulnerable to inactivation and fork locking. This finding highlights the important role of exonuclease activity – the ability to move in reverse protects the fork from inactivation.

DNAP forward translocation promotes fork-locking

The observation that exonuclease activity protects the fork from inactivation suggests that the reverse may also be true: forward translocation could induce fork-locking. To investigate this possibility, we worked with *exo- DNAP*, which showed significant fork-locking after 90 min incubation. To modulate the polymerization rate, we titrated down the nucleotide concentration. We found that under the 12 pN force, the *exo- DNAP* replication rate was about 40 nt/s at 1 mM dNTPs and decreased to 10 nt/s at 5 μ M dNTPs (Fig. 3a,b).

Consistent with our prediction, the inactive fraction diminished with a decrease in dNTPs, from 85% at 1 mM dNTPs to 5% at 5 μ M dNTPs under 90 min incubation (Fig. 3c,d). There is minimal fork-locking behavior at 5 μ M dNTPs. Therefore, these data support the possibility that fork-locking requires DNAP forward translocation. For further confirmation, we replaced the dNTPs with the terminating nucleotides, ddNTPs, which halts replication elongation, and found minimal fork-locking (Fig. 3d).

Collectively, these data show that fork-locking is a consequence of DNAP forward translocation against excessive resistance. Exonuclease activity is essential in minimizing fork

locking by allowing DNAP to move in reverse to alleviate the resistance. Without the exonuclease activity, a persistent forward motion of DNAP against a nearly insurmountable obstacle can lead to DNAP locking the fork by interacting with both the leading and lagging strand, rendering the fork inactive.

Locked replication forks cannot be readily unlocked

The observation that DNAP can lock the replication fork raises the question of whether the fork can be unlocked. We first investigated if DNAP concentration can play a role in this reactivation. We observed a lower inactive fraction and less fork-locking in the presence of 30 nM DNAP versus 1 nM (Fig. 4a). The increase in fork activity suggests that a higher DNAP concentration maintains a more active fork. Inspired by this finding, we investigated whether a higher DNAP concentration could reactivate locked forks. Thus, we incubated the forks under 1 nM DNAP for 90 min, which locked about 15% of the forks, and subsequently introduced 30 nM DNAP to the reaction. We found that the subsequent increase in the DNAP concentration did not reduce the inactive fraction nor the locked fork fraction (Fig. 4a). To further examine this conclusion, we similarly examined *exo*- DNAP and Sequenase activity (Fig. 4a, Fig. S4). Interestingly, an increased concentration of *exo*- DNAP and Sequenase made little difference in preventing fork locking, even at a shorter incubation time. When we incubated the forks with 1 nM *exo*-DNAP, which locked about 85% of the forks, and then subsequently introduced 30 nM WT DNAP to the reaction, we found that the subsequent 30 nM WT DNAP also did not reduce the inactive fraction nor locked fork fraction (Fig. 4a). Taken together, this implies that while excess WT DNAP promotes a more active fork, once the fork becomes locked the excess DNAP cannot facilitate unlocking the fork.

In vivo, helicase arrival at the replication fork could rescue a stalled DNAP as helicase's motor activity may provide the necessary driving force to disrupt the tightly locked fork by DNAP^{3,4}. To investigate this possibility, we slightly revised the experimental approach to improve the data throughput. For this experiment, we used a DNA template with a ssDNA region on the lagging strand to ensure helicase loading (Fig. S1c). We first selected forks locked by WT or *exo*- DNAP during the initial 90-minute incubation period (Methods). Subsequently, we added helicase to the reaction and examined whether helicase could help unlock these forks. We found that helicase was ineffective at reactivating a locked fork (Fig. 4b). The results indicate that the locking configuration is not readily reversible. This finding highlights the importance of the helicase presence at the fork to keep the DNAP from experiencing excessive resistance. If helicase dissociates from the fork, it must be replaced in a timely manner to maintain an active fork.

Discussion

In this work, we discovered that T7 DNAP working alone for an extended duration at a replication fork can tightly lock the replication fork by interacting with both the leading and lagging strand. Fork locking is a consequence of forward DNAP translocation and can be minimized via the exonuclease activity of the DNAP which allows DNAP to move in reverse. Once a fork is locked, it is nearly impossible to reactivate the fork. These findings highlight the importance of the exonuclease activity of the DNAP and the critical need for the presence of helicase at the fork in maintaining an active fork.

In vivo, dNTP concentrations are regulated to be low at 5~37 μM ²⁷. We found that fork locking is a consequence of DNAP forward translocation and is greatly reduced with reduced dNTP concentrations. We speculate this may provide an evolutionary advantage for replication when dNTP concentrations are low. Under this condition, the helicase may dissociate or slip at the fork²⁸, leaving DNAP to work on the fork on its own. The reduced dNTP concentration then minimizes fork locking to maintain an active fork even under sub-optimal growth conditions.

Although our work focuses on the T7 DNAP, our findings may also apply to other prokaryotic DNAPs and eukaryotic DNAPs that replicate the leading strand, such as Pol III of *E. coli* and Pol ϵ of eukaryotes. It is possible that these DNAPs can also lock the replication fork when working on their own. All of these DNAPs contain an exonuclease domain. Although the most well-established role of their exonuclease domains is proofreading²⁹⁻³², recent studies suggest that the ability to degrade the nascent DNA may promote replication restart^{33, 34}. Our findings are consistent with this view and suggest that the exonuclease activity could facilitate fork restart by limiting fork locking and inactivation. In contrast to replicative DNAP, most translesion synthesis (TLS) DNAPs lack the exonuclease function, and usually work in situations in the absence of helicase³⁵. It is possible that TLS DNAPs could also lock the replication fork and must be tightly restricted.

This work demonstrates that maintaining a stable and active replication fork is a complex task, even with the relatively simple T7 system used here. The results and experimental approaches presented here may be applicable to all other replication systems and will facilitate future studies into the complex interactions at the replication fork.

Acknowledgments

We thank members of the Wang Laboratory for helpful discussion and comments. We especially thank Dr. S. Zhang and Biswanath Shaw for some preliminary studies, and T.M. Kay for help with template preparations. This work is supported by the National Institutes of Health grants R01GM136894 (to M.D.W.) and National Institute of General Medical Sciences grant GM118086 (to S.S.P.). M.D.W. is a Howard Hughes Medical Institute investigator.

Author contribution:

X.J., J.T.I, and M.D.W. designed single-molecule assays. X.J. prepared DNA templates. A.S. and S.S.P. purified and characterized T7 gp5_{exo}- and T7 gp4A' proteins. X.J. performed single-molecule experiments and analyzed the data. M.D.W. wrote the initial draft. All authors contributed to the manuscript revision. M.D.W. supervised the project.

COMPETING INTERESTS

The authors declare no competing financial interests.

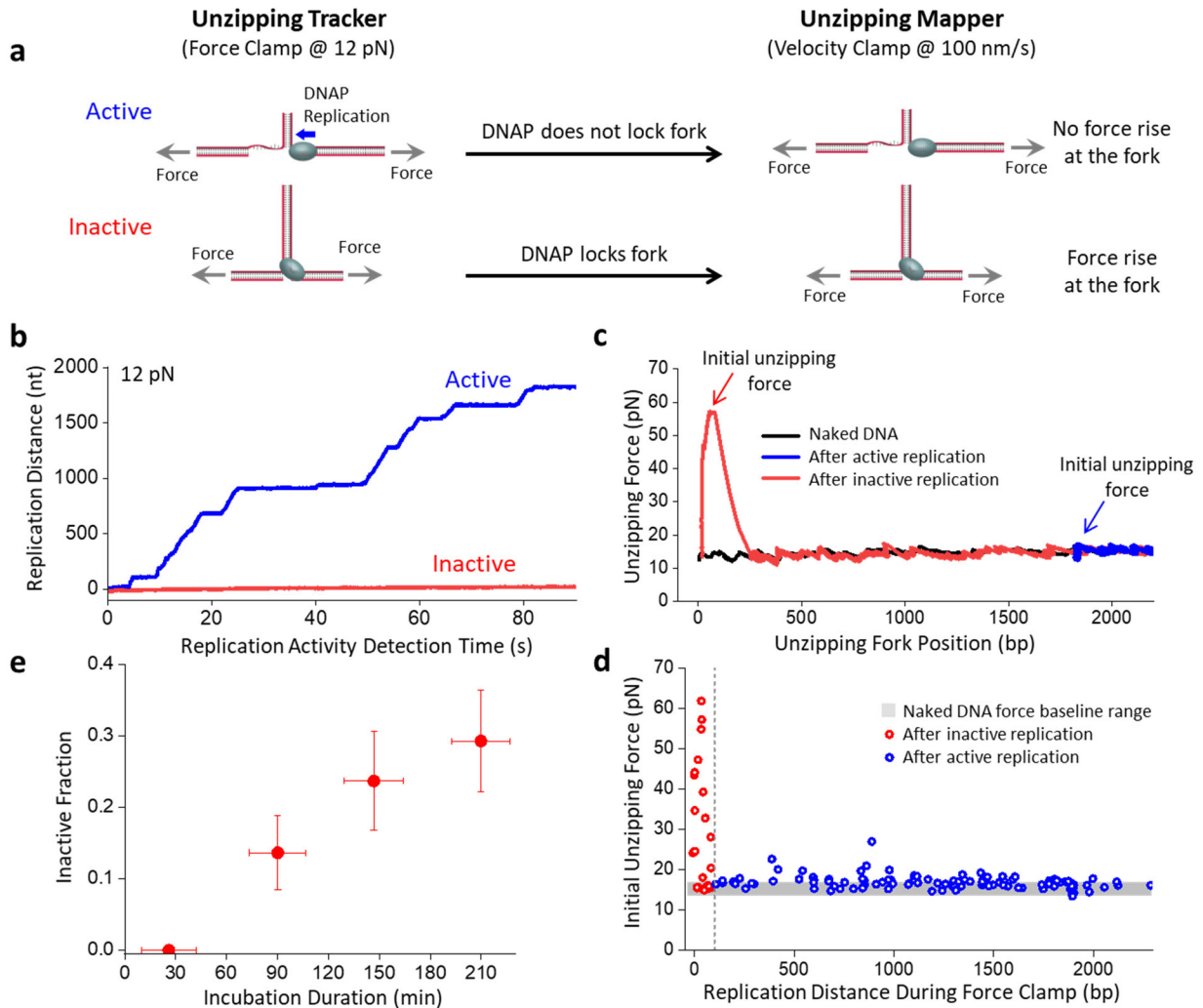


Figure 1. DNAP can lock the replication fork.

a. Experimental techniques for investigating DNAP interactions with replication fork. First, the unzipping tracker uses the DNA fork to track the trajectory of the DNAP in real-time. Active forks held under a constant force result in an increase in the tether extension while inactive forks do not increase the extension. Subsequently, the unzipping mapper detects the location and strength of a bound protein interacting with the fork via mechanical unzipping through the remaining DNA. A locked fork results in a force rise at the start of the unzipping mapper step while an unlocked fork has no detectable force rise.

b. Representative active (blue) and inactive (red) traces during the unzipping tracker step. The replication distance of the DNAP is tracked for 90 s before proceeding to the unzipping mapper step.

c. Immediately after the unzipping tracker step, the unzipping mapper is employed on the same traces shown in **b** to detect any interactions of DNAP with the remaining parental DNA. The unzipping fork position at the start of the unzipping mapper corresponds to the fork position

after replication in the unzipping tracker step. At this initial unzipping fork position, the initial unzipping force indicates resistance to strand opening for the inactive trace (red) and minimal resistance for the active trace (blue). The unzipping mapper curve of naked DNA in the absence of the DNAP is shown in black.

d. The initial unzipping force from the beginning of the unzipping mapper versus the replication distance during the unzipping tracker from $N = 137$ individual traces. Traces identified as active during the replication tracker are shown in blue, and traces identified as inactive in red.

e. The inactive fraction versus incubation duration of DNAP with DNA forks. Error bars represent the standard deviation, with $N = 41, 44, 38,$ and 41 individual traces for 26, 90, 147, and 210 min incubation, respectively.

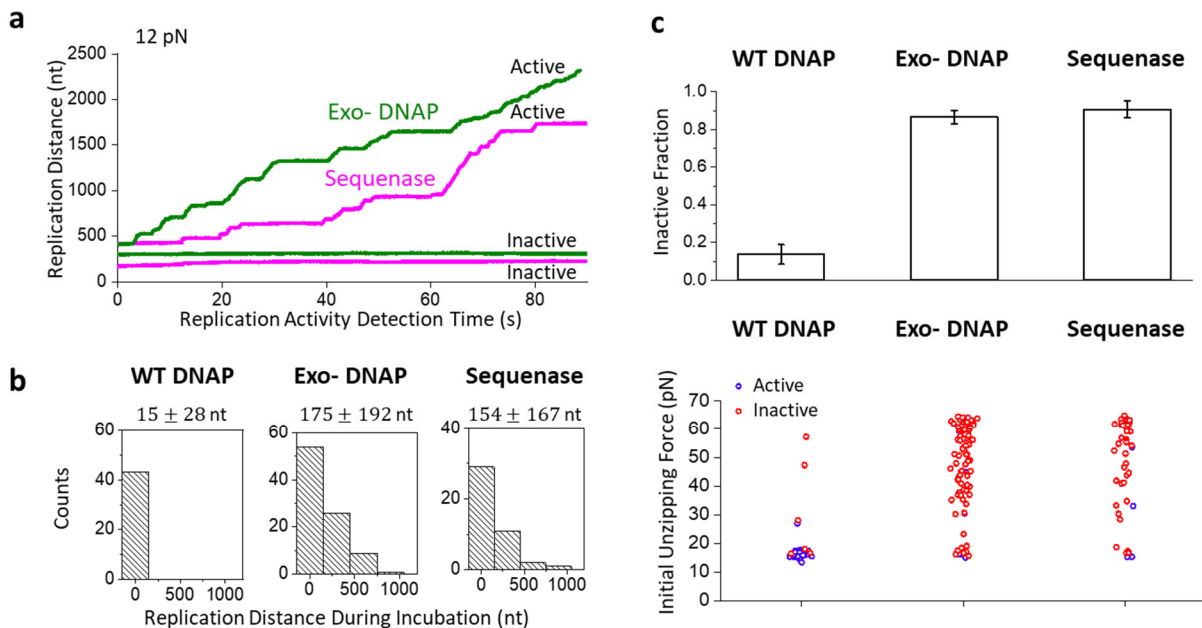


Figure 2. DNAP exonuclease activity limits fork-locking.

The unzipping tracker and unzipping mapper techniques are used to investigate the role of the exonuclease activity of DNAP on fork-locking. Two exonuclease-deficient DNAP mutants, exo- DNAP and Sequenase, are investigated after a 90 ± 17 min incubation with the fork.

a. Representative traces of exo- DNAP (green) and Sequenase (magenta) during the unzipping tracker step.

b. Histograms of the replication distance at the beginning of the unzipping tracker step. The histograms have $N = 43$, 90 , and 43 individual traces for WT DNAP, exo- DNAP, and Sequenase, respectively, with the mean and standard deviation indicated.

c. The inactive fraction and the initial unzipping force of the three DNAPs. Top panel: Error bars represent the standard deviation. The numbers of traces for inactive fractions are the same as in **b**. Bottom panel: The initial unzipping forces have $N = 34$, 87 , and 43 individual traces for WT DNAP, exo- DNAP, and Sequenase, respectively. Active forks are colored blue, and inactive forks are colored red.

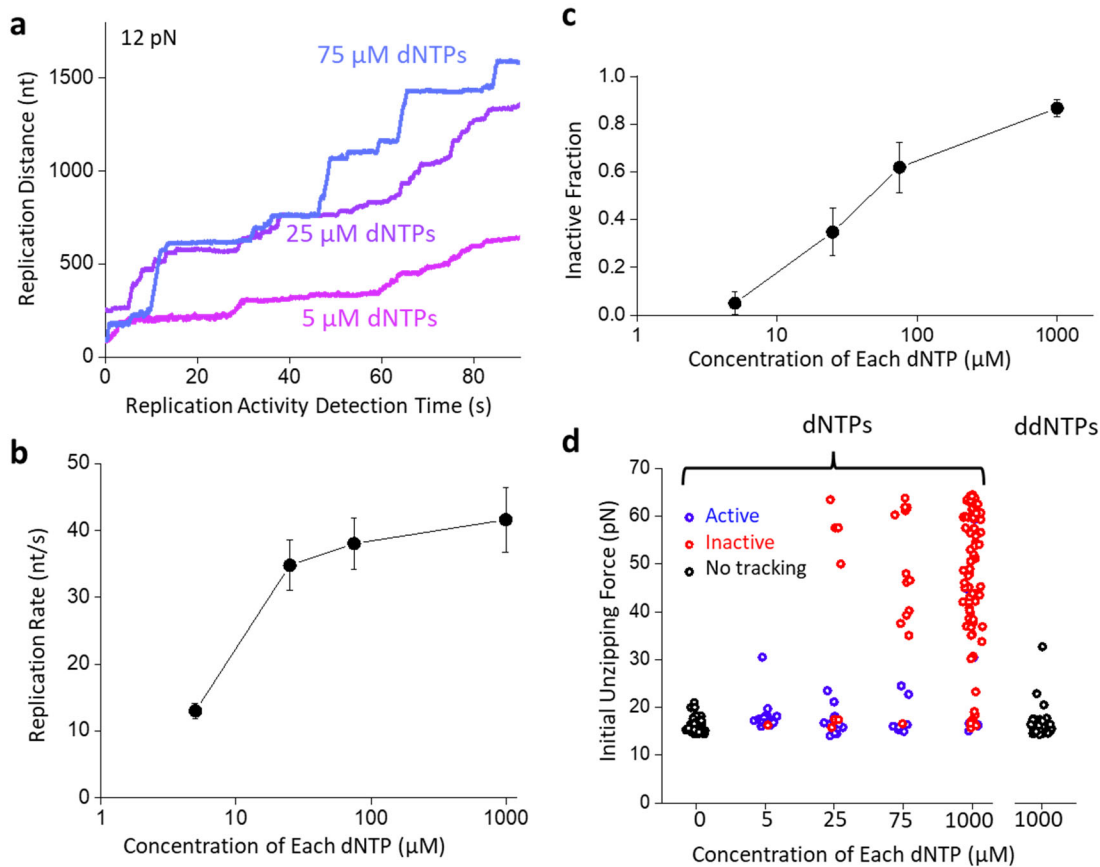


Figure 3. DNAP forward translocation promotes fork-locking

The unzipping tracker and unzipping mapper techniques are used to investigate the role of the forward translocation of DNAP on fork-locking. For these experiments, exo- DNAP was used as it has significant fork-locking activity.

a. Representative traces of exo- DNAP with reduced dNTP concentrations during the unzipping tracker step.

b. Replication rate of the exo- DNAP versus dNTP concentration. Data are from $N = 41, 35, 30,$ and 20 individual traces with 5, 25, 75, and 1000 μ M of each dNTP, respectively. Error bars represent the standard errors of the means.

c. The inactive fraction of the exo- DNAP at different dNTP concentrations, after a 90 ± 17 min incubation with the fork. Error bars represent the standard deviation. Data are from $N = 20, 23, 21,$ and 90 individual traces for 5, 25, 75 and 1000 μ M of each dNTP, respectively.

d. The initial unzipping force of the exo- DNAP at different dNTP concentrations, after a 90 ± 17 min incubation with the fork. Traces that were active during the unzipping tracker are shown in blue, while inactive traces are shown in red, while traces in the absence of dNTPs and with ddNTPS shown in black did not have a tracking step. Data are from $N = 63, 20, 20, 21,$ and 87 individual traces for $0, 5, 25, 75,$ and $1000 \mu\text{M}$ of each dNTP, respectively. The ddNTP $1000 \mu\text{M}$ condition contains $N = 62$ individual traces.

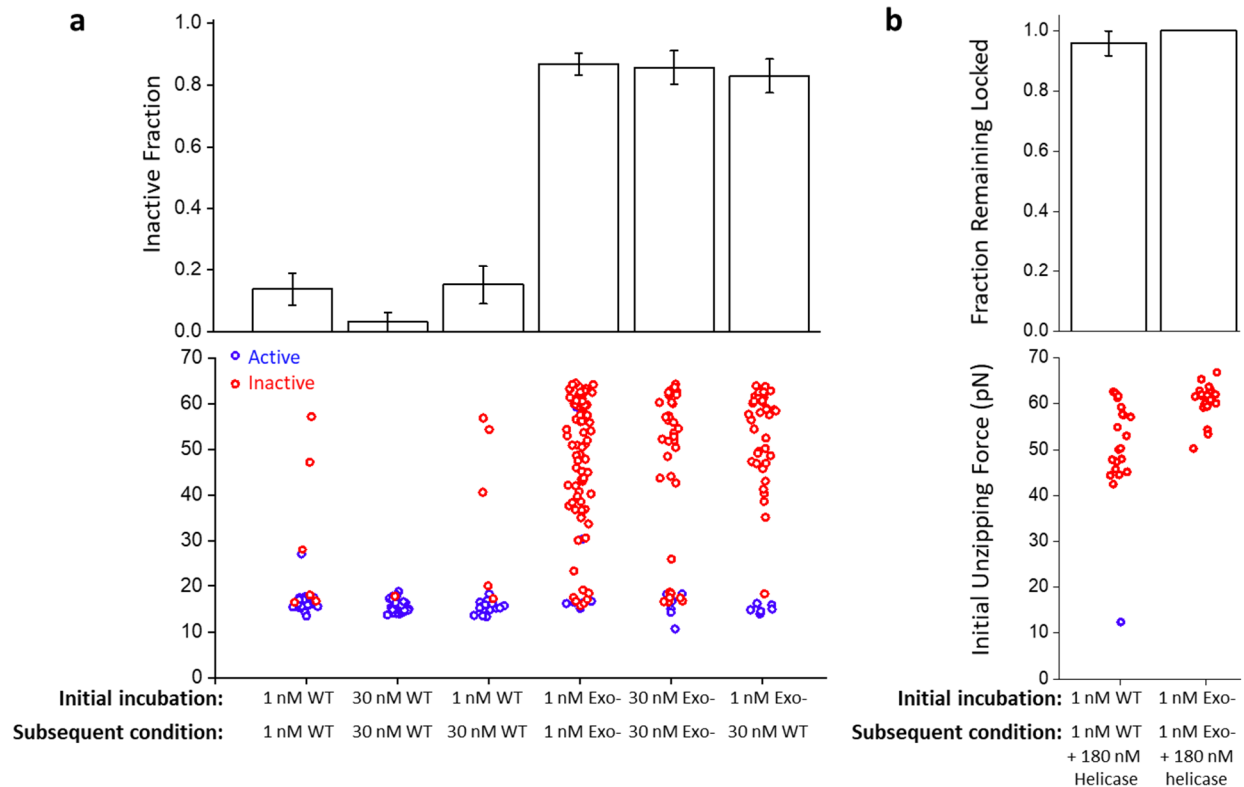


Figure 4. Locked replication forks cannot be readily unlocked.

a. The inactive fraction and initial unzipping force of WT and exo- DNAP under different protein concentrations. Forks were initially incubated with the indicated DNAP type and concentration for 90 min, and subsequently, the DNAP type and concentration were changed to the indicated subsequent condition. Error bars represent the standard deviations. Inactive fraction traces: $N = 44, 33, 33, 90, 42,$ and 48 for conditions shown from left to right. Initial unzipping force traces: $N = 34, 28, 27, 87, 40,$ and 47 for conditions shown from left to right

b. The fraction remaining locked after helicase is introduced to the forks. After the initial incubation of 90 min with WT or exo- DNAP, tethers with locked forks were selected (Methods). After the addition of helicase, these locked forks were checked using unzipping tracker and mapper assays. Reactivated forks are shown in blue, and forks remaining inactive are shown in red. Error bars represent the standard deviations. Fraction remaining locked traces: $N = 24$ and 24 for conditions shown from left to right. Initial unzipping force traces: $N = 22$ and 23 for conditions shown from left to right.

References

1. Hamdan SM, Richardson CC. Motors, Switches, and Contacts in the Replisome. *Annual Review of Biochemistry* 2009, **78**(Volume 78, 2009): 205-243.
2. Nandakumar D, Pandey M, Patel SS. Cooperative base pair melting by helicase and polymerase positioned one nucleotide from each other. *eLife* 2015, **4**: e06562.
3. Sun B, Singh A, Sultana S, Inman JT, Patel SS, Wang MD. Helicase promotes replication re-initiation from an RNA transcript. *Nat Commun* 2018, **9**(1): 2306.
4. Sun B, Pandey M, Inman JT, Yang Y, Kashlev M, Patel SS, *et al.* T7 replisome directly overcomes DNA damage. *Nat Commun* 2015, **6**: 10260.
5. Stano NM, Jeong Y-J, Donmez I, Tummalapalli P, Levin MK, Patel SS. DNA synthesis provides the driving force to accelerate DNA unwinding by a helicase. *Nature* 2005, **435**(7040): 370-373.
6. Pandey M, Patel Smita S. Helicase and Polymerase Move Together Close to the Fork Junction and Copy DNA in One-Nucleotide Steps. *Cell Reports* 2014, **6**(6): 1129-1138.
7. Singh A, Pandey M, Nandakumar D, Raney KD, Yin YW, Patel SS. Excessive excision of correct nucleotides during DNA synthesis explained by replication hurdles. *The EMBO Journal* 2020, **39**(6): e103367.
8. Le TT, Wu M, Lee JH, Bhatt N, Inman JT, Berger JM, *et al.* Etoposide promotes DNA loop trapping and barrier formation by topoisomerase II. *Nat Chem Biol* 2023, **19**(5): 641-650.
9. Le TT, Yang Y, Tan C, Suhanovsky MM, Fulbright RM, Inman JT, *et al.* Mfd Dynamically Regulates Transcription via a Release and Catch-Up Mechanism. *Cell* 2018, **172**(1-2): 344-357.e315.
10. Hall PM, Inman JT, Fulbright RM, Le TT, Brewer JJ, Lambert G, *et al.* Polarity of the CRISPR roadblock to transcription. *Nat Struct Mol Biol* 2022, **29**(12): 1217-1227.
11. Killian JL, Inman JT, Wang MD. High-Performance Image-Based Measurements of Biological Forces and Interactions in a Dual Optical Trap. *ACS Nano* 2018, **12**(12): 11963-11974.
12. Manosas M, Spiering MM, Ding F, Bensimon D, Allemand J-F, Benkovic SJ, *et al.* Mechanism of strand displacement synthesis by DNA replicative polymerases. *Nucleic Acids Research* 2012, **40**(13): 6174-6186.

13. Inman JT, Smith BY, Hall MA, Forties RA, Jin J, Sethna JP, *et al.* DNA y structure: a versatile, multidimensional single molecule assay. *Nano Lett* 2014, **14**(11): 6475-6480.
14. Jin J, Bai L, Johnson DS, Fulbright RM, Kireeva ML, Kashlev M, *et al.* Synergistic action of RNA polymerases in overcoming the nucleosomal barrier. *Nat Struct Mol Biol* 2010, **17**(6): 745-752.
15. Koch SJ, Shundrovsky A, Jantzen BC, Wang MD. Probing protein-DNA interactions by unzipping a single DNA double helix. *Biophysical Journal* 2002, **83**(2): 1098-1105.
16. Koch SJ, Wang MD. Dynamic force spectroscopy of protein-DNA interactions by unzipping DNA. *Physical Review Letters* 2003, **91**(2): 028103.
17. Li M, Hada A, Sen P, Olufemi L, Hall MA, Smith BY, *et al.* Dynamic regulation of transcription factors by nucleosome remodeling. *Elife* 2015, **4**.
18. Hall MA, Shundrovsky A, Bai L, Fulbright RM, Lis JT, Wang MD. High-resolution dynamic mapping of histone-DNA interactions in a nucleosome. *Nat Struct Mol Biol* 2009, **16**(2): 124-129.
19. Shundrovsky A, Smith CL, Lis JT, Peterson CL, Wang MD. Probing SWI/SNF remodeling of the nucleosome by unzipping single DNA molecules. *Nat Struct Mol Biol* 2006, **13**(6): 549-554.
20. Brennan LD, Forties RA, Patel SS, Wang MD. DNA looping mediates nucleosome transfer. *Nat Commun* 2016, **7**: 13337.
21. Whinn KS, Kaur G, Lewis JS, Schauer GD, Mueller SH, Jergic S, *et al.* Nuclease dead Cas9 is a programmable roadblock for DNA replication. *Scientific Reports* 2019, **9**(1): 13292.
22. Doi G, Okada S, Yasukawa T, Sugiyama Y, Bala S, Miyazaki S, *et al.* Catalytically inactive Cas9 impairs DNA replication fork progression to induce focal genomic instability. *Nucleic Acids Research* 2021, **49**(2): 954-968.
23. García-Muse T, Aguilera A. Transcription–replication conflicts: how they occur and how they are resolved. *Nature Reviews Molecular Cell Biology* 2016, **17**(9): 553-563.
24. Engler MJ, Lechner RL, Richardson CC. Two forms of the DNA polymerase of bacteriophage T7. *Journal of Biological Chemistry* 1983, **258**(18): 11165-11173.
25. Lechner RL, Engler MJ, Richardson CC. Characterization of strand displacement synthesis catalyzed by bacteriophage T7 DNA polymerase. *Journal of Biological Chemistry* 1983, **258**(18): 11174-11184.

26. Canceill D, Viguera E, Ehrlich SD. Replication Slippage of Different DNA Polymerases Is Inversely Related to Their Strand Displacement Efficiency*. *Journal of Biological Chemistry* 1999, **274**(39): 27481-27490.
27. Traut TW. Physiological concentrations of purines and pyrimidines. *Molecular and Cellular Biochemistry* 1994, **140**(1): 1-22.
28. Sun B, Johnson DS, Patel G, Smith BY, Pandey M, Patel SS, *et al.* ATP-induced helicase slippage reveals highly coordinated subunits. *Nature* 2011, **478**(7367): 132-U148.
29. Albertson TM, Ogawa M, Bugni JM, Hays LE, Chen Y, Wang Y, *et al.* DNA polymerase ϵ and δ proofreading suppress discrete mutator and cancer phenotypes in mice. *Proceedings of the National Academy of Sciences* 2009, **106**(40): 17101-17104.
30. Reha-Krantz LJ. DNA polymerase proofreading: Multiple roles maintain genome stability. *Biochimica et Biophysica Acta (BBA) - Proteins and Proteomics* 2010, **1804**(5): 1049-1063.
31. Shcherbakova PV, Pavlov YI, Chilkova O, Rogozin IB, Johansson E, Kunkel TA. Unique Error Signature of the Four-subunit Yeast DNA Polymerase ϵ^* . *Journal of Biological Chemistry* 2003, **278**(44): 43770-43780.
32. Hoekstra TP, Depken M, Lin S-N, Cabanas-Danés J, Gross P, Dame RT, *et al.* Switching between Exonucleolysis and Replication by T7 DNA Polymerase Ensures High Fidelity. *Biophysical Journal* 2017, **112**(4): 575-583.
33. Thangavel S, Berti M, Levikova M, Pinto C, Gomathinayagam S, Vujanovic M, *et al.* DNA2 drives processing and restart of reversed replication forks in human cells. *Journal of Cell Biology* 2015, **208**(5): 545-562.
34. Ahmad T, Kawasumi R, Taniguchi T, Abe T, Terada K, Tsuda M, *et al.* The proofreading exonuclease of leading-strand DNA polymerase epsilon prevents replication fork collapse at broken template strands. *Nucleic Acids Research* 2023, **51**(22): 12288-12302.
35. Anand J, Chiou L, Sciandra C, Zhang X, Hong J, Wu D, *et al.* Roles of trans-lesion synthesis (TLS) DNA polymerases in tumorigenesis and cancer therapy. *NAR Cancer* 2023, **5**(1): zcad005.